Tribology and Materials
Vol. 2, No. 4, 2023, pp. 162-171

ISSN 2812-9717
https://doi.org/10.46793/tribomat.2023.020

Experimental and numerical analysis on the thermal performance of the aluminium absorber

Zar Chi LINN *, War War Min SWE, Aung Kyaw SOE, Aung Ko LATT

Mechanical Engineering Department, Mandalay Technological University, Mandalay, Myanmar
*Corresponding author: zarchilinnlinn.mech@gmail.com

Keywords

aluminium
double-pass
solar air collector
temperature
thermal efficiency

History

Received: 01-10-2023
Revised: 22-11-2023
Accepted: 27-11-2023

Abstract

The absorber is a vital part of a solar air collector and has a significant impact on the overall efficiency of a solar air heating unit. The objective of this research is to examine and compare the performance of two distinct aluminium absorbers with and without aluminium fins by using experimental and numerical (computational fluid dynamics – CFD) methods. The studies were conducted in Mandalay, Myanmar, which is located at latitude 21.98° N and longitude 96.1° E, during December 2022. A plate absorber solar air collector (PASAC) and finned absorber solar air collector (FASAC) with the same absorber area of 0.889 m^2 are compared in terms of their thermal performance. At a mass flow rate of 0.0389 kg/s, the average thermal efficiency, as computed numerically, is 53.5 % for FASAC, and the experimental results show a thermal efficiency of 54.2 %. Similarly, for PASAC, the numerical computation yields an average thermal efficiency of 44.4 %, while the experimental results indicate a thermal efficiency of 47.3 %. The FASAC outperforms PASAC in terms of thermal performance. The improved thermal performance of the double-pass solar air collectors with aluminium-finned absorbers can be advantageous for employment as a drying process unit.

1. Introduction

Flat plate solar air collectors are among the most popular nonconcentrated solar thermal collectors because of their simple design and the vast range of application options. Solar air collectors with flat plates for heating air are frequently used in homes for drying laundry, industrial equipment and agricultural fields.

The choice of materials for system components, loads and pre-treatments, temperature of drying obtained in the chamber for drying, flow rate and relative humidity have all been examined to increase the efficiency of solar heating systems [1]. Prioritising improving the layout of the absorbers, increasing the absorber surface and reducing heat loss from the collector would improve the performance and effectiveness of the solar collector [2]. Cross-matrix design is an option because it enables the use of a variety of materials for the heat absorber, which can be advantageous by combining their thermo-physical properties to enhance the performance of the absorber [3]. The low conductance, the air's constrained thermal capacity and the absorption area are only a few of the factors that negatively affect the performance of solar air collectors. Other factors, including heat losses from heat reflection and radiation from components of solar air collectors, may further lower its efficiency [4]. Shetty et al. [5] investigated the effectiveness of a solar collector using a circular-shaped absorbent. They found that the size and quantity of the perforation holes had an impact on the effectiveness of the solar air collector. The findings revealed that the suggested design had the greatest thermal efficiency, at 93 % as opposed to 70 % for standard solar air collectors. Phu and Luan [6] have reported on the properties of thermohydraulic and the effectiveness of the coarse geometry of solar air collector tubes.

The solar air collector's porous materials, a permeable sinuous undulating wire mesh, were researched for thermal performance [7]. MesgarPour et al. [8] constructed a special helical flow configuration across triangular channels and quantitatively investigated it. As a way to demonstrate the mechanism of enhanced heat transfer and the potential for greater efficiency, the outcomes of simulations reveal the distributions of variables within the solar air collector, such as velocity, pressure and temperature. The V-groove expands the turbulent surface area required for greater efficiency, which enhances the transfer of heat from the air to the absorber. The airflow has a significant impact on the efficiency of the collector, which results in a V-groove collector proving more efficient than an ordinary collector with a flat surface of equivalent design [9]. The impact of porous metallic foam on the output of solar collectors was studied mathematically and experimentally by Saedodin et al. [10]. Researchers have suggested several design modifications to boost heat transmission in solar air collectors. Design techniques increase collector thermal transfer surface using finned, reflected and rectangle absorbers [11].

Al-Damook et al. [12] looked at the impact of altering the flow path inside the solar air collector with many passes. A simultaneous flow structure is included in the first approach, a counter-simultaneous flow structure is included in the second and a known U-shape flow arrangement is included in the third. Aluminium cans from recycled sources were fastened to the absorber plate as part of the augmentation procedure. The findings indicated that employing these cans improved all models' thermal efficiency. Additionally, the U-shape performed better thermally than the other shapes. The heat transmission and airflow features of V-shaped rib-roughed solar air collectors were examined numerically by Jin et al. The highest thermohydraulic efficiency factor of 2.35 was determined, owing to the significant enhancement of heat transport by the many V-shaped ribs [13]. In 3D inclination rectangle channels for solar air collectors using natural convection, Kumar and Premachandran quantitatively investigated the impact of atmospheric air on the rate of heat transmission. It is determined that external wind significantly affects the solar air collector channel's flow structure and heat transmission [14].

In the five distinct structures of corrugated and plane solar air collectors examined and researched by Saravanakumar et al. [15], the effect of flow transition dimensions on efficiency, temperature enhancement and pressure drop was investigated. To increase efficiency, arc ribs and baffles were fixed to the absorber plate. The results demonstrated a rise in thermal efficiency of 28.3 % and 27.1 %, respectively, in comparison to the situation without baffles and fins. In order to achieve greater heat transfer coefficients and significantly raise the Nusselt number (Nu) compared to an absorber with no turbulators, Yagnesh Sharma et al. [16] used a plate for absorption containing turbulators. To determine Nu and friction factors, Ravi and Saini [17] carried out an experimental analysis on a double-pass SAC with flat and V-corrugated absorbers. The Nu number for the V-corrugated absorbers increased by 4.5 times in comparison to the flat plate, while the friction factor rose by 3.1.

According to a review of the prior literature, numerous researchers have focused on particular features of double-pass solar air collectors, such as the impact of the number of passes, the shape of the fins and absorber materials on performance. In this study, double-pass solar air collectors are constructed and tested for the effect of black-coating flat plate aluminium absorbers with and without black-coating aluminium fins as part of an experimental assessment. The primary advantages of using fins are clearly shown in this system, one of which is the increased heating effect brought on by increased collector surface utilisation. Simulation work was also done for the thermal system of the complete model, which produces findings that are competitive with the experimental one. The effects of other factors, such as air mass flow rate, airflow behaviour, air temperature distribution, etc. on thermal performance were also studied.

2. Material and method

Due to improvements in the efficiency of solar collectors, several nations are now urging researchers to create these systems in order to get the most out of them as a source of heating independent of conventional fuel. The solar collector system affixed to the absorber surface with and without fins was studied. The city of Mandalay, Myanmar, which is situated at a longitude of 96.1° E, a latitude of 21.98° N and an elevation of 22 m above sea level, was the site of

practical experiments. Experiments were conducted in December 2022 in the period from 9:00 to 17:00.

The review of existing literature revealed that the materials required for constructing a highly effective solar absorber plate are generally costly to acquire or integrate. Typically, the absorbing plate is constructed from materials known for their high thermal conductivity, such as copper, aluminium, etc. to maximise the transfer of heat to the target fluid. Copper possesses greater conductivity than aluminium. Nonetheless, copper is pricier and has a higher density compared to aluminium. Therefore, the primary objective is to create an economically efficient absorber plate to fulfil the objectives of this study. The key challenges involve ensuring the durability and thermal efficiency of the absorber plate, as well as managing the costs associated with the materials. This paper concentrated on the utilisation of aluminium materials and coatings to maximise the efficiency of the absorber plate while keeping costs at a minimum.

2.1 Collector absorber material

The absorber plate and fins are typically manufactured from materials with high thermal conductivity, such as aluminium, to be able to transmit the most heat to the intended fluid. The following advantages of aluminium make it suitable for use in this work and make it a vital component.

Aluminium oxidises rapidly, and a layer of aluminium oxide that forms as a result prevents further corrosion from occurring from air, water and chemicals. This protective layer is transparent, colourless and stain-resistant. Anodising makes it simple to colour aluminium and it keeps painting quite well. Different methods can be used to finish aluminium. Aluminium is completely recyclable and retains all of its original properties. The strength-to-weight ratio of aluminium is good. Aluminium is a great material option for uses where magnetism must be avoided. Aluminium is an exceedingly light material.

Aluminium has a high thermal conductivity of 238 W/mK, which helped disperse thermal energy throughout the material during the initial development of the absorber material and increased the quantity of solar radiation that was converted to thermal energy [18]. The thermal diffusivity value of aluminium, which is 9.7×10^{-5} m^2/s, is an important factor in evaluating the performance of solar thermal absorbers and their suitability for thermal energy storage [19,20].

The black paint coating on the aluminium metal was applied using a liquid spray-on method. The coating material is ATM A 210 Spray Acrylic Lacquer in black, specially formulated from high-quality acrylic resin and nitrocellulose. It provides an exceptional property of quick drying. It is easy to paint with aerosol to give a colourful and glossy finish. It has excellent adhesion to every substrate, like metal, plastic and wood. The air vapour pressure of this aerosol paint spray is 4.5 – 5 kg/cm^2 at 30 °C. The surface of the aluminium metal plate was first thoroughly cleaned to remove dirt, rust and grease by using some chemicals such as NaOH, HCl and distilled water, and then dried. The paint was sprayed on the cleaned aluminium plate surface at ambient temperature. The drying time for the first coating was about 15 minutes. The coating thickness of about 89 – 95 μm was obtained, and it was checked by using a paint thickness meter LS220 (Linshang). Using a flat black coating modifies the radiative properties of a surface, increasing the transmissivity and absorptivity of the solar thermal absorber surface while decreasing its reflectivity. These characteristics are crucial to the solar thermal absorber because they can greatly improve the rate of heat transfer between the absorbent substance and the air.

2.2 Energy efficiency

To assess the thermal effectiveness of the existing solar air collector design, a calculation will be made. The average temperatures of the air are used for estimating the parameters of the output. Additionally, the effectiveness parameters are influenced by the characteristics of the atmosphere, which alter with variations in the flux of radiation from the sun. The output parameters relating to the thermal efficiency of the double-pass solar air collectors are calculated as in [21].

The useful heat gain is

$$Q_u = \dot{m} c_p (T_{f,out} - T_{f,in}), \quad (1)$$

where $\dot{m}$ is the mass flow rate of air, c_p is the specific heat capacity of air and $T_{f,in}$ and $T_{f,out}$ are the inlet and outlet air temperatures.

The mass flow rate of air is

$$\dot{m} = \rho u A, \quad (2)$$

where ρ is the density of the air, u is the velocity of the air and A is the area of the airflow channel.

The thermal efficiency of an air collector is defined as

$$\eta = \frac{Q_u}{IA_c}, \quad (3)$$

where I is the intensity of the solar irradiance and A_c is the area of the solar collector.

2.3 Experimental setup

Two identical solar air collectors with various black-coated aluminium absorber surfaces were created with the same parameters, operated under the same weather conditions and exposed to various air velocities. The first is a finless double-pass flat plate aluminium absorber solar air collector and the second has 18 finned flat plate aluminium absorber on the upper flow channel of the collector. The fins are arranged transversely to induce a large turbulent flow, thereby enhancing the heat transfer rate and extending the length of the airflow path.

The rectangular box-shaped structure of the solar air collector is made from a 1.27 cm thick plywood sheet. A 4 mm thick glass covering is placed over the channel on top to block longwave radiation from leaking into the environment while permitting the solar absorber to receive the maximum amount of solar energy. The absorber plates of the collectors were constructed from 2 mm thick aluminium plates and coated in black. It was possible to achieve more accurate findings from experiments by lowering the loss of heat from double-pass solar air collectors by insulating the collectors with foam.

Double-pass solar air collectors have been put to the test at the same tilt angle of 45 degrees. The real tilt angle is 37 degrees which is obtained by adding 15 to the latitude of 22 in winter for Mandalay, Myanmar. However, for the midday sun, which is the hottest on short winter days, it should be steeper by 8 to 10 degrees, which is why a 45 degree tilt angle is chosen in this study. Fins are employed in the flow path to modify the absorber of the collector components and are made of the same material and thicknesses (2 mm thick aluminium). There are 18 fins in the upper flow channel as shown in Figure 1. An air fan (12 V, 0.24 A) is used to feed air to the solar air collector. The tests are carried out on similar increments of mass flow rates of air between 0.0194 and 0.0389 kg/s. K-type thermocouples are used for measuring the temperature at various locations, and their readings are recorded. The investigations involved using an anemometer to determine air velocity. Figure 2 displays the side measurements of the collector, as well as the placements of the fins.

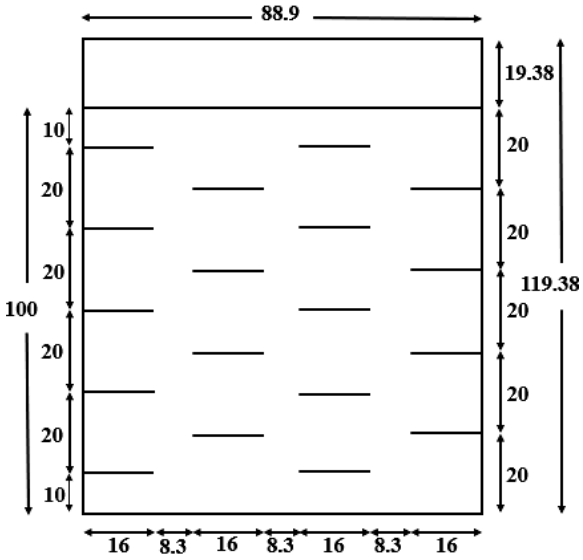

Figure 1. Plan view of the upper flow channel of FASAC (dimensions are in cm)

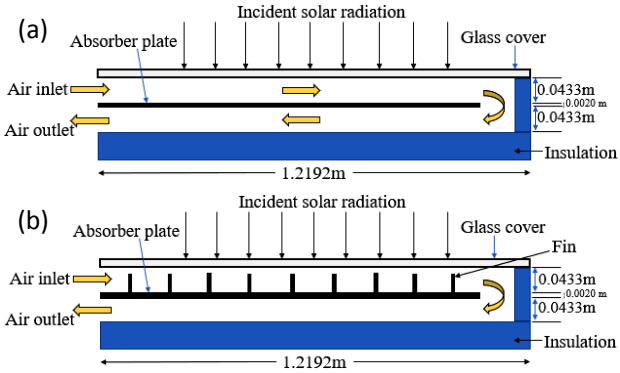

Figure 2. A schematic side view of double-pass solar air collector: (a) PASAC and (b) FASAC

The materials utilised in the experimental setup, along with the dimensions and other details of the solar air collector setups, are presented in Table 1. Table 2 provides the details and accuracy of the measuring instruments applied in the experiments. Table 3 displays the properties of the main materials employed in the simulation [7,22,23].

2.4 Experimental procedure

The covers of the collectors were cleaned before the trials began, and after being transported to the testing location, the collectors were operated for ten minutes to start the procedure. At this time, all of the instruments used for measurement were checked. At the start of the testing at 09:00 AM, the first experiment was run for two collectors at the

Table 1. Specifications and dimensions of solar air collector

Component	Material	Parameter	Dimension
Transparent cover	glass	length width thickness	1.2192 m 0.9144 m 0.0040 m
Absorber plate	aluminium	length width thickness	1.0000 m 0.8890 m 0.0020 m
Insulator	foam	length width thickness	1.1938 m 0.8890 m 0.0127 m
Cover box (floor)	plywood	length width thickness	1.1938 m 0.8890 m 0.0127 m
Cover box (side)	plywood	length width height	1.2192 m 0.9144 m 0.1200 m
Air channel (upper/lower)	air	length width height	1.1938 m 0.8890 m 0.0433 m
Fin	aluminium	length width thickness	0.1600 m 0.0333 m 0.0020 m

Table 2. Specifications of measuring apparatus

Equipment	Model	Usage	Accuracy
Solar power meter	Tenmars TM-206	Measuring solar intensity	± 5 %
Digital thermometer	Elitech DS-1	Measuring temperatures	± 1 °C
Anemometer	Lutron AM 4201	Measuring velocity	± 2 %

Table 3. Properties of the main materials

Material	Density, kg/m^3	Specific heat capacity, J/kgK	Thermal conductivity, W/mK
Aluminium	2710	900	238
Glass	2500	840	1.0500
Foam	23	1131	0.0350
Air	1.059	1007	0.0281
Copper	8900	390	398

same mass flow rate of 0.0194 kg/s for six minutes. The second experiment was then conducted for the same time interval with a mass flow rate of 0.0215 kg/s, and so on for all ten mass flow rates. Up until the experiment's conclusion, ambient conditions were considered and documented every six minutes. For the ten mass flow rates, the experiments were tested for one hour and eight times were tested for eight hours per day. The average of eight values is calculated for each mass flow rate result throughout the day. Following that, the results of each mass flow rate are received. The solar meter was positioned parallel to the collector cover to get a precise reading.

3. Numerical analysis

3.1 Geometry and meshing

The two configurations are generated using the CFD application Ansys CFX. The geometry of the two combinations is handled by an Ansys workbench-developed modeler. These two configurations contained the glass cover, the absorber with and without fins, the air domain and the thermal insulator. Figure 3 displays the developed configurations.

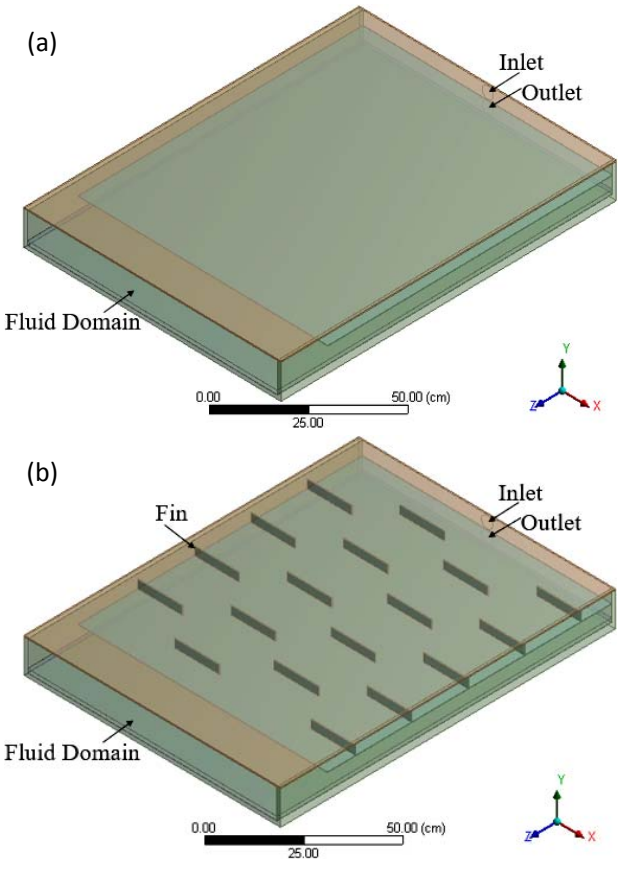

Figure 3. Geometry of the configuration: (a) first configuration and (b) second configuration

The mesh is generated both inside the volume and at the interface between the fluid and solid domains. CFD is the preferred analysis method in physics. The largest and smallest face sizes are 150

mm and 7.52 mm, respectively. There are roughly 2.3 million elements and 1.7 million nodes in the system. The K-epsilon turbulence model is shown to be reliable for free-shear flows and to distribute uniform air flow rates in the air channel of the collector. Surface and volume meshing are done using tetrahedron meshing, which is seen in Figure 4. The maximum skewness value in this meshing is less than 0.9 and the average value is 0.3.

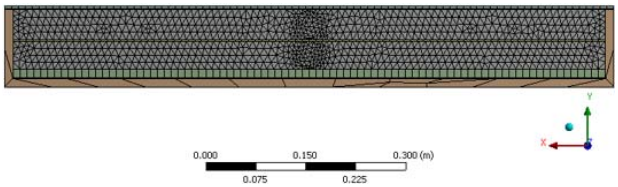

Figure 4. Meshing of the double-pass collector

3.2 Boundary conditions

Table 4 shows the boundary conditions of the double-pass collectors. Air enters the inlet of the solar collector and leaves through the outlet.

Table 4. Boundary conditions of the collector

Boundary condition	Value
Solar irradiance, W/m^2	894.4 (average)
Mass flow rate × 10^{-3}, kg/s	19.4, 21.5, 23.7, 25.9, 28.1, 30.2, 32.4, 34.6, 36.8, 38.9
Inlet air temperature, °C	25 (average)
Air velocity, m/s	1

A plywood and foam adiabatic wall with no sliding characteristics forms the wall border. The air domain is transferring heat to the glass. The heat transfer option of the fluid model is thermal energy. The K-epsilon turbulence model is used. The turbulent flow Prandtl number is 0.7202.

4. Results and discussion

The numerical analysis is finished using the mass flow rates that were employed as input in the experimental study after the collector has undergone an experimental inquiry. Thermal efficiency is improved in double-pass solar air collectors that use fins on the absorber of the air route as opposed to double-pass solar air collectors without fins. Rectangular fins are affixed to the absorber plate within the air channel to induce turbulence in the airflow. Incorporating fins in the air channel not only decreases the Nusselt number but also, by reducing the hydraulic diameter and inducing airflow turbulence, enhances the heat transfer coefficient from the absorber plate to the airflow. This consequently leads to a reduction in total heat loss and higher outlet air temperatures [24]. This may be due to the fins' huge surface area for heat transfer and, as a result, their high volumetric heat transfer coefficient. The air moving through the first air route in the counterflow system absorbs heat from the upper channel before moving through the second channel.

4.1 Experimental results

The impact of mass flow rate on output temperature with and without fins is depicted in Figure 5. As the air flow rate is increased, temperature differences get smaller. Additionally, the output temperature is higher when fins are used than when they are not because fins have a larger surface area for heat transmission and higher thermal conductivity.

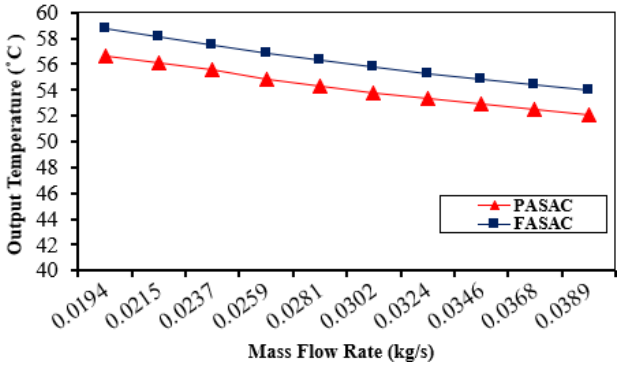

Figure 5. Effect of mass flow rate on output temperature of the flat plate and finned absorber double-pass collector (experimental results)

The maximum output temperature in the double-pass collector at 0.0194 kg/s of mass flow rate was 58.8 °C when fins were used, while it was 56.6 °C when fins were not used. When utilising fins, the maximum temperature difference of the double-pass collector was 18.8 °C, whereas when using a flat plate absorber, it was 16.6 °C at a mass flow rate of 0.0194 kg/s.

Although the outlet air temperature is lower than other values at a mass flow rate of 0.0389 kg/s, the maximum useful energy of 539.8 W has been achieved by the finned absorber collector. This is primarily due to the dominating effect of the Reynolds number, which leads to an increase in the convective heat transfer rate, thereby capturing more thermal energy from the surface of the solar absorber. Figure 6 displays the results of thermal efficiency measurements as a function of

mass flow rates for double-pass solar collectors with and without fins. As the mass flow rate increases, the thermal efficiency of the collector also increases. Due to the use of fins, which increases the region that transfers heat and causes the temperature to rise, efficiency increases as the temperature does.

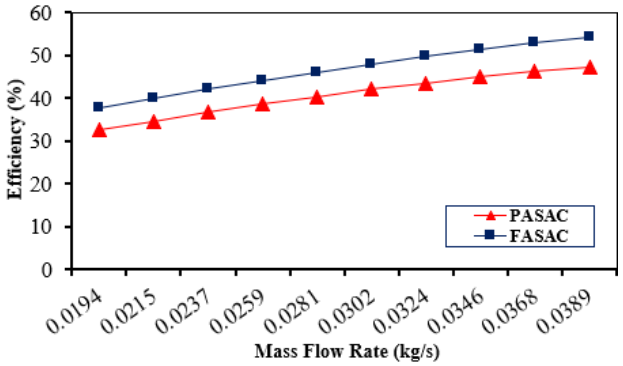

Figure 6. Effect of mass flow rate on the thermal efficiency of the flat plate and finned absorber double-pass collector (experimental results)

As an experimental result, efficiency increases while using the double-pass mode since more heat is removed. It is notable that the double-pass collector at 0.0389 kg/s yields the experiment's maximum thermal efficiency, which is 54.2 %. As the air flow rate increased from 0.0194 to 0.0389 kg/s, the system's thermal efficiency climbed to 54.2 % and 47.3 % with double-pass collectors with and without fins. The average thermal effectiveness of the finned absorber plate double-pass collector increases by 7 % when compared to a double-pass collector without fins. Hence, using fins improves the area for heat transfer, leading to improved thermal efficiency.

4.2 Simulation results

By providing input air temperature measurements for one-hour time intervals, a CFD model is examined for the location of Mandalay Technology University in December 2022 from 9:00 to 17:00. The outlet condition has been used to compare the CFD model to the experimental model.

Figures 7a and 7b show the temperature contours of the air domain for double-pass collectors at a lower mass flow rate of 0.0194 kg/s. They depict temperature variation for outlet airflow through the lower side of the double-pass air collector for PASAC and FASAC. Similarly, Figures 7c and 7d show temperature contour plots of the double-pass solar air collector fluid zone at the mass flow rate of 0.0281 kg/s. The temperature contour for the same configuration at the greater mass flow rate of 0.0389 kg/s is given in Figures 7e and 7f as a comparison. The temperature contour plot is measured using the same coordinate in pictures for all the various mass flow rates. In those figures, as the mass flow rate increases, the temperature decreases. Five points were measured at the outlet of the collectors for each airflow rate to determine the average temperature.

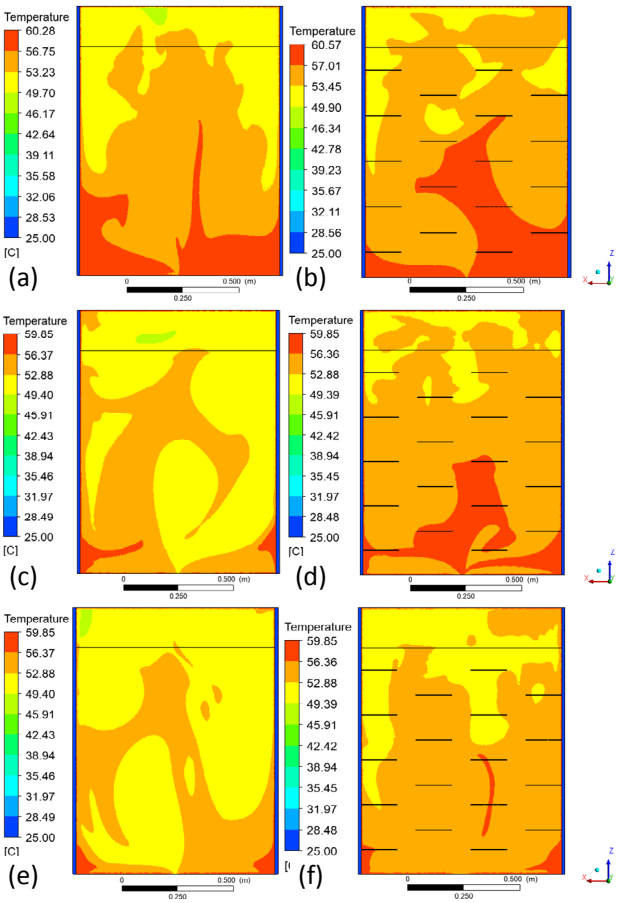

Figure 7. Temperature distribution of the lower side of the double-pass solar air collector with and without fins in the simulation: (a) PASAC at 0.0194 kg/s, (b) FASAC at 0.0194 kg/s, (c) PASAC at 0.0281 kg/s, (d) FASAC at 0.0281 kg/s, (e) PASAC at 0.0389 kg/s and (f) FASAC at 0.0389 kg/s

The heat transmission from the absorber plate to the fluid flow is improved by using the finned absorber, which optimises contact surface area. Figure 8 illustrates how the output temperature decreases for different absorber plates as the air flow rate rises from 0.0194 to 0.0389 kg/s. At a mass flow rate of 0.0194 kg/s, the finned absorber of the double-pass collector reaches outlet temperatures of 58.4 °C, whereas the absorber surface of the double-pass collector without fins reaches outlet temperatures of 56.1 °C. For a variety

of mass flow rates under investigation, a declining change in temperature was seen when the mass flow rate increased from 0.0194 to 0.0389 kg/s.

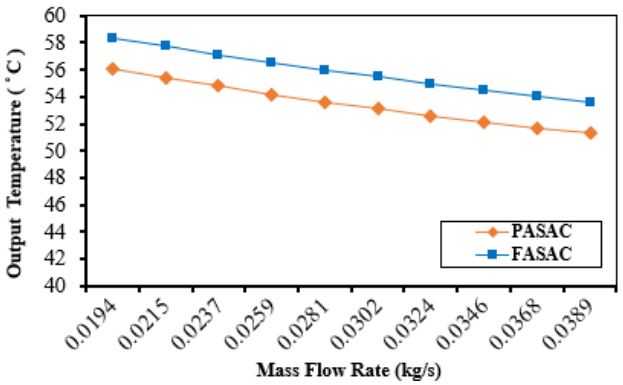

Figure 8. Variation of output temperatures with mass flow rates for double-pass collectors (numerical results)

Under the same boundary condition, the double-pass collector without fins absorbers falls from 56.1 to 51.3 °C, while the finned absorber of the double-pass collector falls from 58.4 to 53.6 °C. A crucial factor in improving convective heat transfer rate is the absorber surface geometry, which enhances the heat exchanger's effective surface area and capacity to absorb solar radiation. Convective heat transmission to the flowing fluid is substantially influenced by the absorber area.

According to Figure 9, thermal efficiency rises when the mass flow rate increases from 0.0194 to 0.0389 kg/s. Reduced collector heat loss and the use of a finned absorber can increase thermal efficiency. At 0.0194 kg/s, the thermal efficiency was 36 %, and 31.4 %, as to 0.0389 kg/s, it increased to 53.5 % and 44.4 % with fins and without fins double-pass collectors.

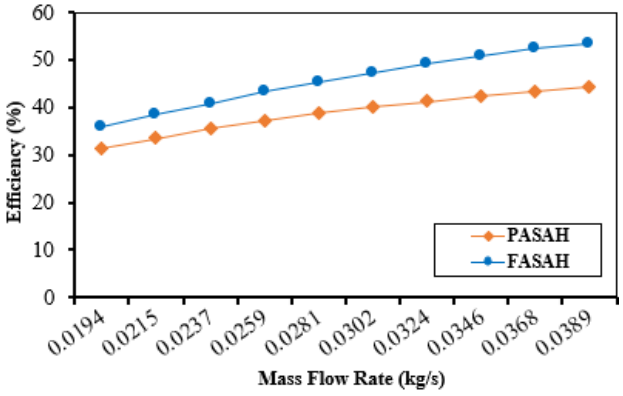

Figure 9. Effect of mass flow rate on thermal efficiency for different absorber plates (numerical results)

When compared to a double-pass collector without fins, the finned absorber plate double-pass collector increases efficiency by 9.1 %. This is because internal convective heat exchangers improve with increased airflow while maintaining a constant heat loss. Less energy is indeed required to overcome friction loss at a lower mass flow rate. As the mass flow rate increases, the friction loss increases sharply, increasing the energy needed to overcome it. It is important to find the ideal flow and keep it constant because, in this analysis, mass flow rates lower than 0.0194 kg/s and higher than 0.0389 kg/s were not taken into consideration.

The simulation also involved the use of a copper absorber to assess the efficiency of materials in this study. Figure 10 presents the comparative results between aluminium and copper absorbers. According to the simulation findings, copper is 0.4 % more efficient without fins and 1.2 % more efficient with fins compared to the aluminium absorber.

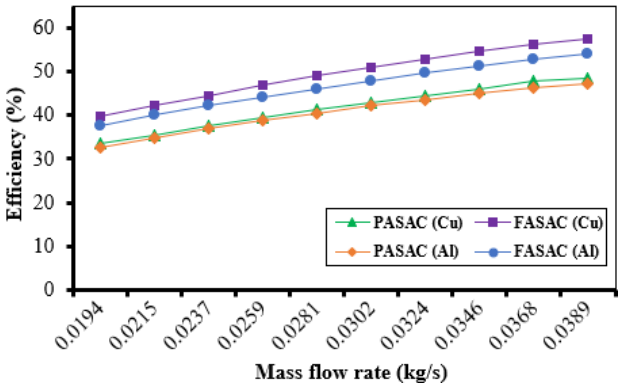

Figure 10. Effect of mass flow rate on thermal efficiency for copper (Cu) and aluminium (Al) absorber plates (numerical results)

4.3 Validation of work

An experimental analysis of double-pass solar air collectors is carried out. Results from the experimental investigation are contrasted with those from the CFD simulation. Figure 11 compares the efficiency of the experimental investigation and the CFD simulation study. The greatest average deviation for the efficiency between the numerical and experimental values of the finned absorber collector is ± 1.9 % and that of the flat plate absorber collector is ± 4.9 %, respectively. Readings can vary within reasonable bounds.

According to the experimental data, the thermal efficiency can be increased in double-pass collectors by utilising fins by 54.2 % and by 47.3 % when fins are not used. Finally, the efficiency variation shown in Figure 11 for a mass flow rate in double-pass mode under both experimental and numerical settings shows that efficiency increases as the mass flow rate increases.

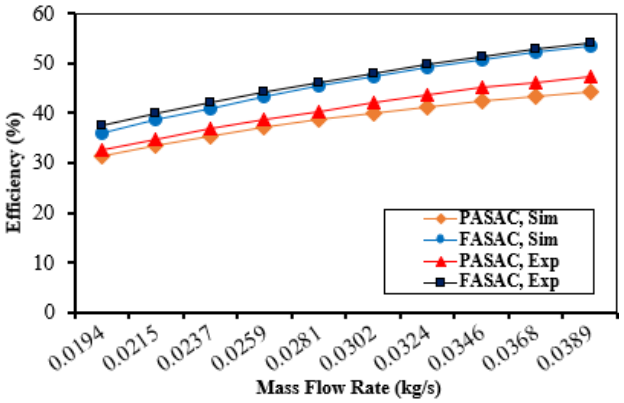

Figure 11. Comparison between experimental (Exp) and simulated (Sim) values of efficiency

The thermal efficiency of flat plate and finned absorber solar air collectors was compared with experimental values for thermal efficiency obtained by Karim and Hawlader [25]. Figure 12 shows the comparison of the analytical with experimental results. The average deviation of thermal efficiency of flat plate absorber and finned absorber collectors are ± 7.3 and ± 6.6 % from the experimental values of Karim and Hawlader. This indicates a good agreement with experimental results, ensuring the accuracy of the data obtained by mathematical modelling.

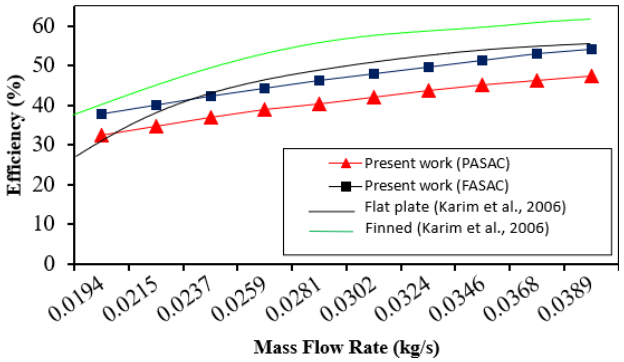

Figure 12. Comparison of the thermal efficiency of flat-plate and finned absorber solar air collectors based on available experimental results

5. Conclusion

The output of the collector can be developed using numerous techniques. Therefore, the best way to increase thermal efficiency is to emphasise the selection of absorber material and the dual advantages of using fins. The surface area of the absorber plate is increased by the addition of fins, which also enhances the amount of heat it absorbs. Additionally, the inclusion of fins causes turbulence to be more intense, which improves the combination of cold and hot air. The performance of the collectors is improved by these actions.

Experimental and numerical data, including with and without aluminium fins absorber plates of double-pass solar air collectors, are given and analysed. An experimental setup was established in order to investigate the effects of using different aluminium absorber plates on the efficiency of double-pass solar air collectors. Ansys CFX is used to explore the computational fluid dynamics of double-pass solar air collectors.

The finned aluminium absorber collector was found to be more effective in this analysis. At the type of double-pass collector with aluminium fins, the maximum efficiency and the temperature difference were achieved as 54.2 % and 19 °C, respectively.

The output temperature range of the study is from 54 to 58.8 °C, which is required for a variety of agricultural drying applications. From the experimental results, adding aluminium fins to the aluminium absorber plate of the collector is a viable method for improving the thermodynamic performance of the collector. The improved thermal effectiveness of the double-pass solar air collectors with finned aluminium absorbers can be advantageous for employment as a drying process unit.

References

[1] H. El Hage, A. Herez, M. Ramadan, H. Bazzi, M. Khaled, An investigation on solar drying: A review with economic and environmental assessment, Energy, Vol. 157, 2018, pp. 815-829, DOI: 10.1016/j.energy.2018.05.197

[2] G. Colangelo, E. Favale, P. Miglietta, A. de Risi, Innovation in flat solar thermal collectors: A review of the last ten years experimental results, Renewable and Sustainable Energy Reviews, Vol. 57, 2016, pp. 1141-1159, DOI: 10.1016/j.rser.2015.12.142

[3] Z.A.A. Majid, A.A. Razak, M.H. Ruslan, K. Sopian, Characteristics of solar thermal absorber materials for cross absorber design in solar air collector, International Journal of Automotive and Mechanical Engineering, Vol. 11, 2015, pp. 2582-2590, DOI: 10.15282/ijame.11.2015.36.0217

[4] H. Hassan, S. Abo-Elfadl, Experimental study on the performance of double pass and two inlet ports solar air heater (SAH) at different configurations of the absorber plate, Renewable Energy, Vol. 116, No. A, 2018, pp. 728-740, DOI: 10.1016/j.renene.2017.09.047

[5] S.P. Shetty, A. Paineni, M. Kande, N. Madhwesh, N. Yagnesh Sharma, K. Vasudeva Karanth, Experimental investigations on a cross flow solar

air heater having perforated circular absorber plate for thermal performance augmentation, Solar Energy, Vol. 197, 2020, pp. 254-265, DOI: 10.1016/j.solener.2020.01.005

[6] N.M. Phu, N.T. Luan, A review of energy and exergy analyses of a roughened solar air heater, Journal of Advanced Research in Fluid Mechanics and Thermal Sciences, Vol. 77, No. 2, 2021, pp. 160-175, DOI: 10.37934/arfmts.77.2.160175

[7] S. Singh, Experimental and numerical investigations of a single and double pass porous serpentine wavy wiremesh packed bed solar air heater, Renewable Energy, Vol. 145, 2020, pp. 1361-1387, DOI: 10.1016/j.renene.2019.06.137

[8] M. MesgarPour, A. Heydari, S. Wongwises, Geometry optimization of double pass solar air heater with helical flow path, Solar Energy, Vol. 213, 2021, pp. 67-80, DOI: 10.1016/j.solener.2020.11.015

[9] A. Fudholi, K. Sopian, B. Bakhtyar, M. Gabbasa, M.Y. Othman, M.H. Ruslan, Review of solar drying systems with air based solar collectors in Malaysia, Renewable and Sustainable Energy Reviews, Vol. 51, 2015, pp. 1191-1204, DOI: 10.1016/j.rser.2015.07.026

[10] S. Saedodin, S.A.H. Zamzamian, M. Eshagh Nimvari, S. Wongwises, H. Javaniyan Jouybari, Performance evaluation of a flat-plate solar collector filled with porous metal foam: Experimental and numerical analysis, Energy Conversion and Management, Vol. 153, 2017, pp. 278-287, DOI: 10.1016/j.enconman.2017.09.072

[11] K. Kashyap, R. Thakur, A. Kumar, Mathematical simulation of performance evaluation of different types of baffle shapes solar air heater, JP Journal of Heat and Mass Transfer, Vol. 16, No. 2, 2019, pp. 221-243, DOI: 10.17654/HM016020221

[12] M. Al-Damook, Z.A.H. Obaid, M. Al Qubeissi, D. Dixon-Hardy, J. Cottom, P.J. Heggs, CFD modeling and performance evaluation of multipass solar air heaters, Numerical Heat Transfer, Part A: Applications, Vol. 76, No. 6, 2019, pp. 438-464, DOI: 10.1080/10407782.2019.1637228

[13] D. Jin, S. Quan, J. Zuo, S. Xu, Numerical investigation of heat transfer enhancement in a solar air heater roughened by multiple V-shaped ribs, Renewable Energy, Vol. 134, 2019, pp. 78-88, DOI: 10.1016/j.renene.2018.11.016

[14] D. Kumar, B. Premachandran, Effect of atmospheric wind on natural convection based solar air heaters, International Journal of Thermal Sciences, Vol. 138, 2019, pp. 263-275, DOI: 10.1016/j.ijthermalsci.2018.12.010

[15] P.T. Saravanakumar, D. Somasundaram, M.M. Matheswaran, Thermal and thermo-hydraulic analysis of arc shaped rib roughened solar air heater integrated with fins and baffles, Solar Energy, Vol. 180, 2019, pp. 360-371, DOI: 10.1016/j.solener.2019.01.036

[16] N. Yagnesh Sharma, N. Madhwesh, K. Vasudeva Karanth, The effect of flow obstacles of different shapes for generating turbulent flow for improved performance of the solar air heater, Procedia Manufacturing, Vol. 35, 2019, pp. 1096-1101, DOI: 10.1016/j.promfg.2019.06.062

[17] R.K. Ravi, R.P. Saini, Nusselt number and friction factor correlations for forced convective type counter flow solar air heater having discrete multi V shaped and staggered rib roughness on both sides of the absorber plate, Applied Thermal Engineering, Vol. 129, 2018, pp. 735-746, DOI: 10.1016/j.applthermaleng.2017.10.080

[18] Y.A. Çengel, Introduction to Thermodynamics and Heat Transfer, McGraw-Hill, Dubuque, 2008.

[19] Y.A. Çengel, J.M. Cimbala, R.H. Turner, Fundamentals of Thermal-Fluid Sciences, McGraw-Hill Education, New York, 2012.

[20] Thermal diffusivity table, available at: https://www.engineersedge.com/heat_transfer/thermal_diffusivity_table_13953.htm, accessed: 01.09.2023.

[21] J.A. Duffie, W.A. Beckman, Solar Engineering of Thermal Processes, John Wiley & Sons, Hoboken, 2013, DOI: 10.1002/9781118671603

[22] Glass – Density – Heat capacity – Thermal conductivity, available at: https://material-properties.org/glass-density-heat-capacity-thermal-conductivity, accessed: 26.05.2021.

[23] Y.A. Çengel, M.A. Boles, Thermodynamics: An Engineering Approach, McGraw-Hill Education, New York, 2015.

[24] A. Daliran, Y. Ajabshirchi, Theoretical and experimental research on effect of fins attachment on operating parameters and thermal efficiency of solar air collector, Information Processing in Agriculture, Vol. 5, No. 4, 2018, pp. 411-421, DOI: 10.1016/j.inpa.2018.07.004

[25] M.A. Karim, M.N.A. Hawlader, Performance investigation of flat plate, v-corrugated and finned air collectors, Energy, Vol. 31, No. 4, 2006, pp. 452-470, DOI: 10.1016/j.energy.2005.03.007